Preliminary Analyses of Volcanic Tremor Associated with 1992 Eruptions of Crater Peak, Mount Spurr Volcano, Alaska

By Stephen R. McNutt, Guy C. Tytgat, and John **A.** Power

CONTENTS

ABSTRACT

The occurrence of volcanic tremor played an important role in monitoring and eruption forecasting at Mount Spurr by signifying changes in rates of precursory seismicity and indicating the beginnings and ends of eruptions. For example, the onset of continuous tremor provided the principal basis for changing the level of concern color code 15 hours before the first eruption on June 27, 1992. The onset of strong tremor marked the beginning of each of the three main eruptions, and it was the basis for issuing updates and notifications The declines in tremor amplitude signaled the ends of the eruptions. Tremor also provided physical insight concerning eruptive processes based on spatial and temporal variations in amplitudes and frequencies versus time. The volcano is monitored by a network of 10 seismic stations within 22 km of the vent, in addition to regional seismic stations at greater distances. Three types of tremor were observed at Mount Spurr in association with the 1992 eruptions—tremor bursts lasting 1 to 10 minutes, continuous tremor lasting 2 hours to several days, and tremor during eruptions. Tremor bursts occurred from June 6 to 26 in higher numbers at first which then declined. The overall cumulative energy curve is concave upward, but individual segments are all concave downward; this phenomenon suggests that sources of energy such as heat or water formed quickly then gradually lost energy. Tremor energy increased by one order of magnitude in the **3** days before the first eruption on June 27, 1992. Comparison of spectra from June 26 and June 27 showed that spectral peaks were shifted to lower frequencies by 18 percent; this shift suggests an increase in source length or a decrease in velocity caused perhaps by formation of bubbles. RMS amplitude ratios computed for near (400 m) and far *(5* km) stations showed an increase by a factor of 2.7 at the near station from June 11 to June 25, which we model as a shoaling of the source depth. Eruption tremor was substantially stronger than any of the pre-eruption tremor, and was recorded on stations at distances of as much as 138 km. Calculated reduced displacements ranged from 16 to 30 cm^2 for the strongest eruption tremor. The duration of the strongest eruption tremor was crudely proportional to the tephra volume for the three eruptions. Future efforts will focus on modeling the source mechanisms in greater detail.

INTRODUCTION

Active volcanoes produce a great variety of seismic signals. In addition to earthquakes and various low-frequency events, volcanic tremor is often observed. The typical appearance of tremor is that of an irregular sinusoid, and a key distinguishing feature is its long duration compared with earthquakes of the same amplitude. Continuous signal durations of days, weeks, and longer are common. Tremor has been recorded at 129 volcanoes worldwide (McNutt, 1992).

Volcanic tremor has received considerable attention in the literature over the past few years. Research efforts have been concentrated in four main areas: (1) sources, including shock-waves, (2) propagation effects, **(3)** magma flow and bubble distribution, and (4) nonlinear models. Theoretical work on tremor by Chouet (1992) focused chiefly on source effects of fluid pressurization in resonant cavities excited by a variety of mechanisms. Chouet numerically treated a rectangular crack that was excited by pressure pulses

acting at various locations on the surface of the crack. He considered his source model to apply to both long-period (LP) events and to volcanic tremor, by assuming that superposition of LP events produced tremor. More recently, Chouet and others (1994) have extended this model to the LP swarms accompanying the 1989–90 eruptions of Redoubt Volcano, Alaska. They suggest, in the new model, flow-induced shock waves at a depth of 1.4 km below the vent as the source of the pressure pulses. Dawson and others (1992) modeled a small, low-velocity zone at the same depth, and they suggested the presence of a small magma body.

Gordeev (1992) studied propagation effects, using near-surface pressure fluctuations such as explosions as sources, and he modeled waveforms propagating through low-velocity layers overlying a half space. His conclusion was that the frequencies and waveforms of tremor are chiefly caused by propagation effects. Hurst (1992) performed stochastic simulations of tremor using both white noise and Poisson forcing functions to excite resonance in a simple harmonic oscillator. He also allowed the oscillator to have a random damping factor. His simulations produced synthetic signals that closely resemble observed volcanic tremor at Ruapehu in New Zealand.

Montalto and others (1992) qualitatively modeled the effects of bubble distribution on tremor and eruption energy for the 1990 eruptions of Mount Etna in Sicily. They suggest that low-amplitude tremor is caused by bubbly flow of magma, whereas high-amplitude tremor is caused by slug flow.

Ukawa (1993) made an important observation for the 1989 Ito-oki submarine eruption. He found that low-frequency (1 Hz) tremor within 50 km of the source consisted primarily of surface waves trapped in sedimentary layers. Middle-frequency tremor (2–7 Hz) observed at the same time at more distant stations was composed primarily of body waves, thus highlighting the importance of propagation effects. Julian (1994) studied a nonlinear model for tremor generation, using a lumped parameter model of flow through a channel that is represented by a mass-spring system, which includes damping. He argued that self-oscillations of this system can produce most of the main features observed in volcanic tremor. In summary, all this recent work suggests that a variety of source and propagation effects are present in volcanic tremor, and there is as yet no consensus about the tremor source. In fact, there are such a variety of observations and source models that there are probably several sources for tremor, not just one.

The occurrence of volcanic tremor played an important role in eruption monitoring and forecasting at Mount Spurr by signifying changes in rates of precursory seismicity and indicating the beginnings and ends of eruptions. For example, the onset of continuous tremor provided the principal basis for changing the level of concern color code 15 hours before the first eruption on June 27, 1992. The onset of strong tremor marked the beginnings of each of the three main eruptions, and it was the basis for issuing updates and notifications. The declines in tremor amplitude signaled the ends of the eruptions. Analyses of tremor helped provide insight into physical processes that occurred prior to, during, and after the three eruptions of June 27, August 18, and September 16–17, 1992. Three types of volcanic tremor were recorded at Mount Spurr: (1) tremor bursts of 1 to 10 minutes duration, with irregular amplitudes, occurring from June 6 to June 26; (2) continuous tremor lasting 2 hours to several days, with uniform amplitudes, occurring June 24–27, September 17–25, October 2–20, and November 9–10; and (3) tremor during eruptions on June 27, August 18, and September 16–17. The purpose of this paper is to show examples of all three types of tremor and to present results from the preliminary analyses that have been performed as of April 1993. We also discuss possible models for tremor at Mount Spurr, compare its tremor to that at other volcanoes, and discuss the role played by tremor in eruption forecasting.

MOUNT SPURR TREMOR DATA

Mount Spurr is monitored by a network of 10 seismic stations within 22 km of the summit (fig. 1). The active vent, Crater Peak, is located 400 m west of seismic station CPK. Eight of the stations have a 1-Hz vertical geophone, (CPK and CPA are three-component) and data are telemetered in analog form via radio and microwave to the Alaska Volcano Observatory offices at the Geophysical Institute of the University of Alaska Fairbanks. Power and others (this volume) describe the instrumentation and various data-acquisition systems in detail. One data-acquisition system used in Fairbanks digitizes the signals at a sampling rate of 120 samples per second using a Masscomp computer system. In addition to triggered event recording, this system records data continuously from about 140 stations of the Alaska regional seismic network 24 hours per day on DAT tapes (Sonnafrank and others, 1991). This computer provided the primary data set analyzed in this paper. Seismic data are also recorded on a Real-time Seismic Amplitude Measurement (RSAM) system (Endo and Murray, 1991), a Seismic Spectral Amplitude Measurement (SSAM) system (Stephens and others, 1994), and on a PC/AT computer, which runs continuously in event-detected mode (Lee, 1989).

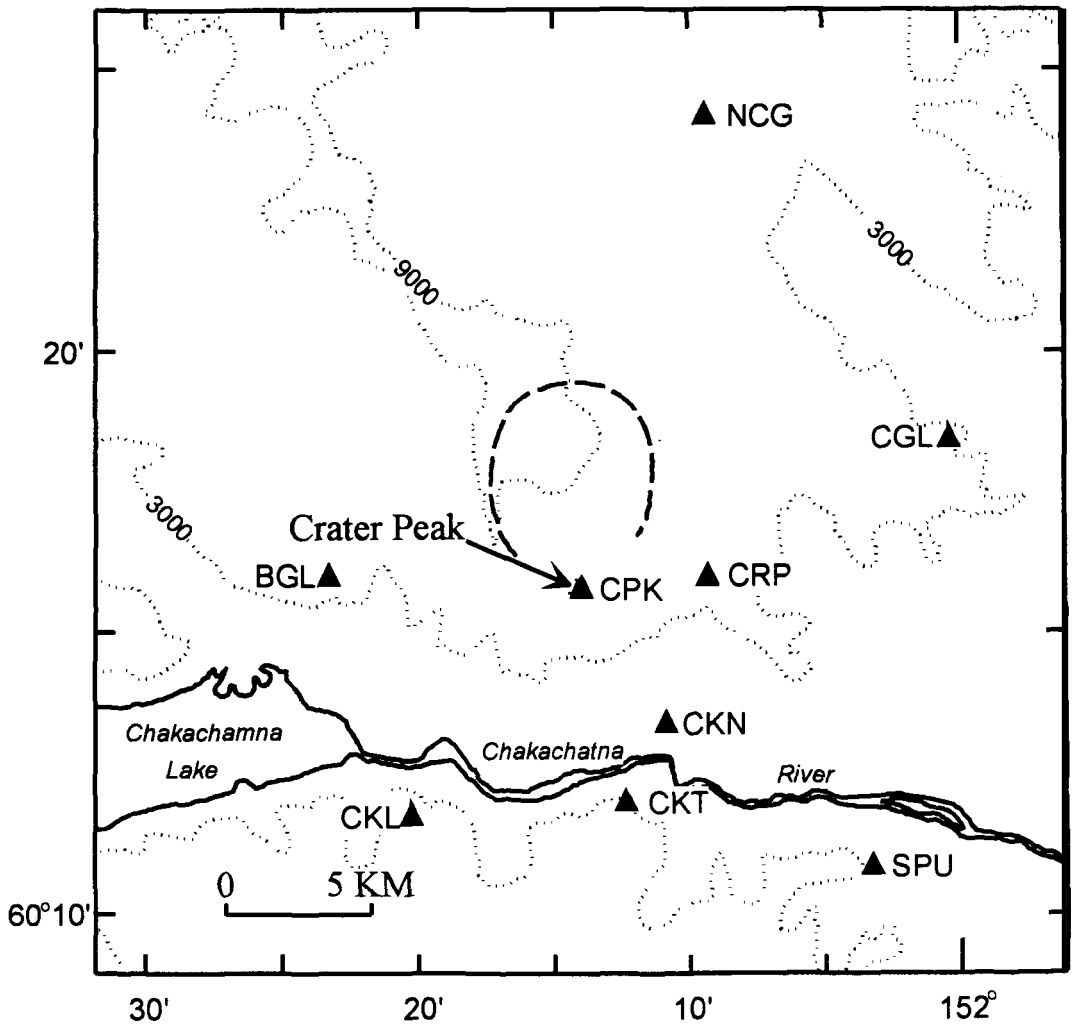

Figure 1. Seismic stations within 20 km of Mount Spurr volcano, southwestern Alaska. Station CPK was destroyed 46 minutes after the start of the June 27, 1992, eruption and was reinstalled in early September. Station CPK was destroyed again on September 17 and was replaced by station CP2. Station CRP became inoperative about 2 hours after the start of the August 18 eruption, and was repaired several days later. Dashed line is caldera boundary. Contours in feet.

Both RSAM and SSAM are rapid-analysis tools used routinely by the Alaska Volcano Observatory. RSAM provides plots of 1-minute averages of seismic amplitude or energy, and SSAM provides plots of spectral amplitude in predetermined narrow frequency bands. Both of these monitoring tools are useful for quantitatively determining the gross features of tremor automatically during crises when detailed manual analyses are not possible. RSAM and SSAM are especially useful digital recording techniques when signal amplitudes on helicorder drums begin to overlap or exceed the physical dynamic range of analog recording, and so reliable amplitudes cannot be easily obtained. At Mount Spurr, RSAM and SSAM were most useful during tremor episodes on June 26–27, October 1–6, and November 9–10.

Volcanic tremor first appeared at Mount Spurr on June 6, 1992, following a 9.5-month swarm of volcano-tectonic earthquakes (Power and others, this volume). The tremor appeared as irregular events 1 to 10 minutes in duration, and had relatively high amplitudes at station CPK (400 m from the vent; CPK- is a co-located low-gain station) and lower amplitudes at other stations (fig. 2). Dominant frequencies were between 3 and 6 Hz at station CPK, and about 2 Hz at other stations. We called the events tremor bursts on the basis of their similarity to events recorded at other volcanoes, such as Mammoth Mountain (Hill and others, 1990). We use the term "bursts" for tremor lasting 1 to 10 minutes and the term "episodes" for tremor lasting hours or longer. The only tremor with durations between 10 minutes and 1 hour was associated with eruptions on August 18 and September 16–17.

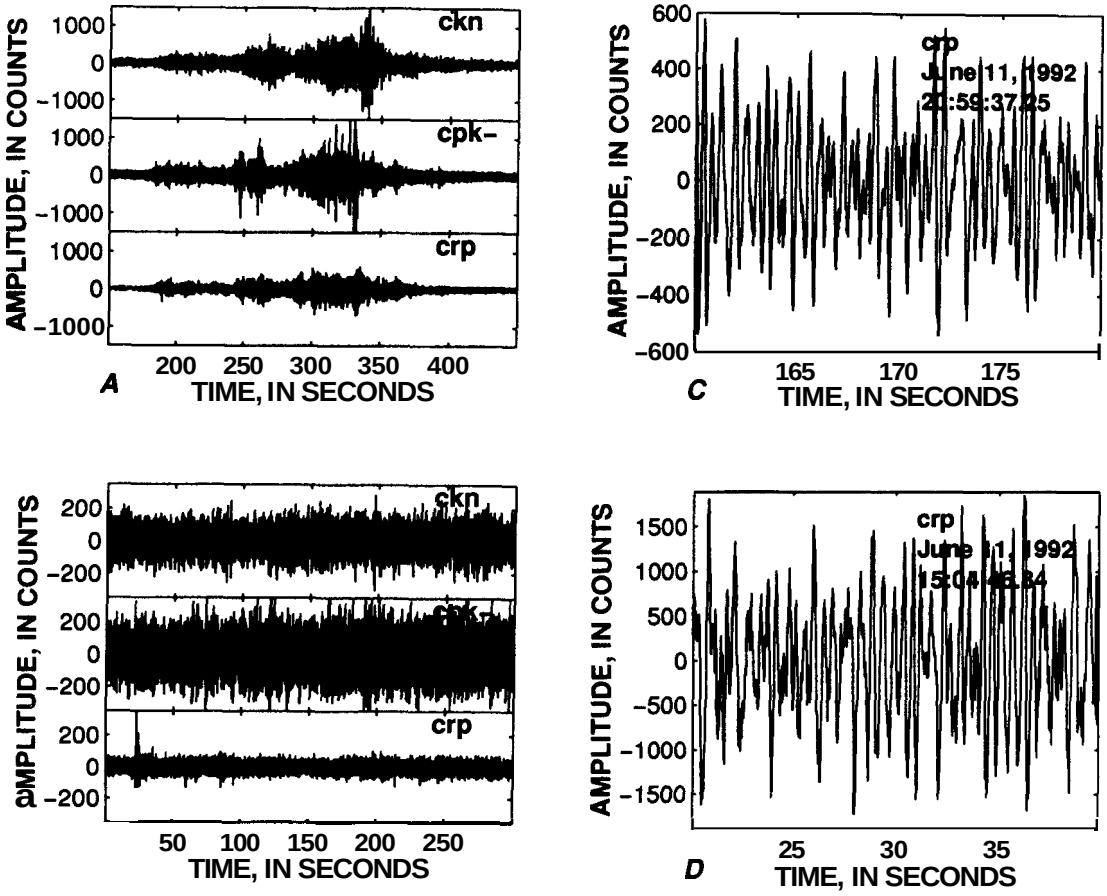

Figure 2. Seismograms of volcanic tremor from Mount Spurr volcano, Alaska. **A**, tremor burst from June 11, **1992,** on stations **CKN, CPK,** and **CRP,** 300 sec of data shown; B, tremor episode June **24–25, 1992,** same 3 stations, 300 sec of data shown; C, continuous tremor from June **26, 1992,** station **CRP, 20** sec of data shown; D, eruption tremor, June **27, 1992,** station **CRP, 20** sec of data shown.

A total of 174 tremor bursts occurred between June 6 and June 27 (Appendix 1). A peak rate of 24 tremor bursts occurred on June 11, and one burst each occurred on June 17, 18, and 21. We measured durations in seconds for each event on seismograms from station CPK, and peak-to-peak amplitudes in mm on seismograms from station CRP because CPK was frequently saturated (see Appendix 1). Squaring the amplitude and multiplying by the corresponding duration of each burst gave a measure of relative energy. We then summed the durations and energies for each 6-hour period. The resulting plots of cumulative durations and energy rates were approximately constant from June 6 to June 13, then declined (became less steep) until June 21, when they increased slightly (fig. 3). On June 24, a 154-minute long tremor episode occurred, followed 12 hours later by another similar episode lasting 142 minutes. Continuous tremor began at 12:03 p.m. ADT (20:03 UT) on June 26 and lasted 19 hours until the onset of the eruption on June 27 at 07:04 a.m. ADT (15:04 UT). The amplitude fluctuated during this time (fig. 4) and the signal resembled banded tremor (Kieffer, 1984; McKee and others, 1981). The three tremor episodes from June 24–27 represented an order of magnitude increase in energy over all the tremor bursts recorded until June 24 (fig. 3). Tremor amplitude approximately doubled on June 27, 1992, at 07:04 a.m. ADT (15:04 UT), signaling the start of the eruption. This was recognized within 2 minutes, and the level of concern color code was formally changed several minutes later.

Being able to consistently determine eruption start times, end times, and durations (table 1) precisely was problematic because of station failures. Start times were determined as the time when the amplitude on the station CRP helicorder in Fairbanks first exceeded 3 mm peak-to-peak (1.5 mm peak to-peak for September owing to a gain change). On, June 27, this occurred about 12 seconds after the apparent start of the eruption on station CPK, which was the closest station, located on the crater rim 400 m from the vent. The 12-sec delay was partly due to propagation time

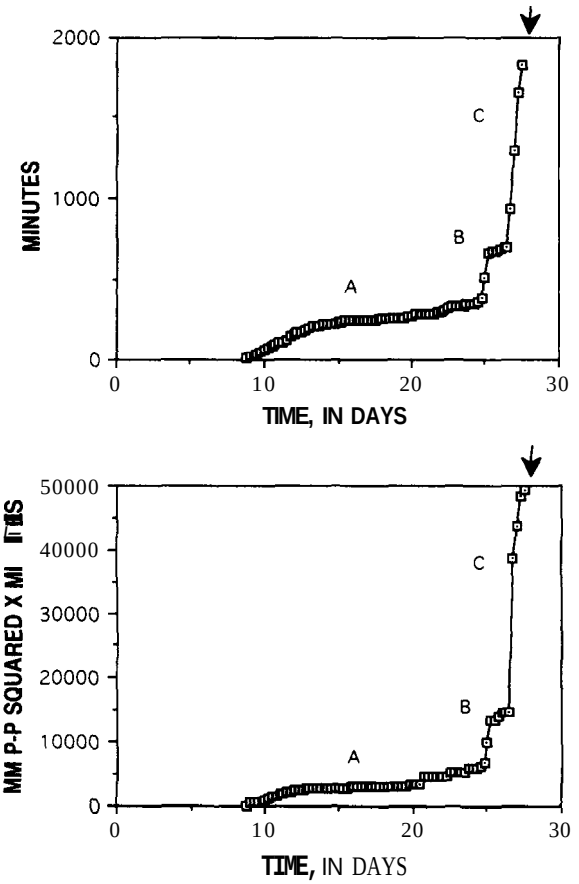

Figure 3. Mount Spurr tremor cumulative duration and energy versus time for June 1992. Data computed for 6-hour intervals. Eruption occurred on June 27 (arrows). The energy units are mm squared times minutes, and differ from standard units such as ergs by a multiplicative constant. Parts labeled A, B, and C are discussed in text.

and partly due to attenuation at the 5-km distance of station CRP. Unfortunately, station CPK was destroyed, so it could not be used to determine the start times for all the eruptions, so station CRP was used instead. The end times were determined when the peak-to-peak amplitude on the station BGL helicorder in Fairbanks dropped below 1 mm (2 mm for September). This is a fairly high threshold because of the greater distance of station BGL (7.7 km), so the indicated times correspond to the strong phases of activity. Station BGL was used for end times because station CRP became inoperative after a lightning strike during the eruption on August 18. All times and durations are shown in table 1.

This first eruption lasted 4 hr and 3 min (table 1). No tremor was recorded over the next 52 days until August 18, when a 12-minute burst of weak tremor including 3 entrained LP events coincided with pilot reports of a small ash plume. About 1 hour later, the main phase of the second eruption began, accompanied by strong tremor (as much as 30 cm^2 reduced displacement) lasting 3 hr and 28 min. No tremor was recorded over the next 29 days until September 16, about 3 hours before the September 16–17 eruption. Medium-strength tremor (maximum about 5 cm2 reduced displacement) occurred for 11 min during the first phase of the eruption at 10:36 p.m. ADT, and strong tremor (as much as 25 cm^2 reduced displacement) occurred for 3 hr and 36 min during the main phase of the eruption which began at 12:03 a.m. ADT September 17 (table 1). Unlike the aftermath of the June 27 and August 18 eruptions, continuous tremor occurred for 1 week following the September 17 eruption.

Tremor reappeared on October 2, and it occurred almost continuously with variable amplitude until October 20. The last tremor occurred during a swarm of earthquakes on November 9–10, 1992, that may have been associated with an intrusion (Stephens and others, unpub. data).

Altogether, during the 1992 activity of Mount Spurr, more than 460 hours of volcanic tremor were recorded.

Table 1. Mount Spurr volcano, Alaska, eruption start times, end times, and durations, as determined from tremor amplitudes, for 1992 eruptions.

[All times expressed in Alaskan daylight time.]

Date	Start time CRP>3mm	End time BGL<1mm	Duration hr:min	Tephra volume[A] $x10^3 m^3$
6/27	07:04:49 a.m.	11:07:51 a.m.	4:03	44
8/18	03:41:06 p.m.	03:52:55 p.m.[#]	0:12	(visible ash plume)
8/18	04:42:25 p.m.	08:10:45 p.m.	3:28	52
9/16	10:36:18 p.m.	10:47:40 p.m.[*]	0:11	(2-km ash plume)
9/17	12:03:48 a.m.	03:39:52 a.m.	3:36	56

^ R. McGimsey, written commun., 1993

measured at station CRP

* BGL<2mm

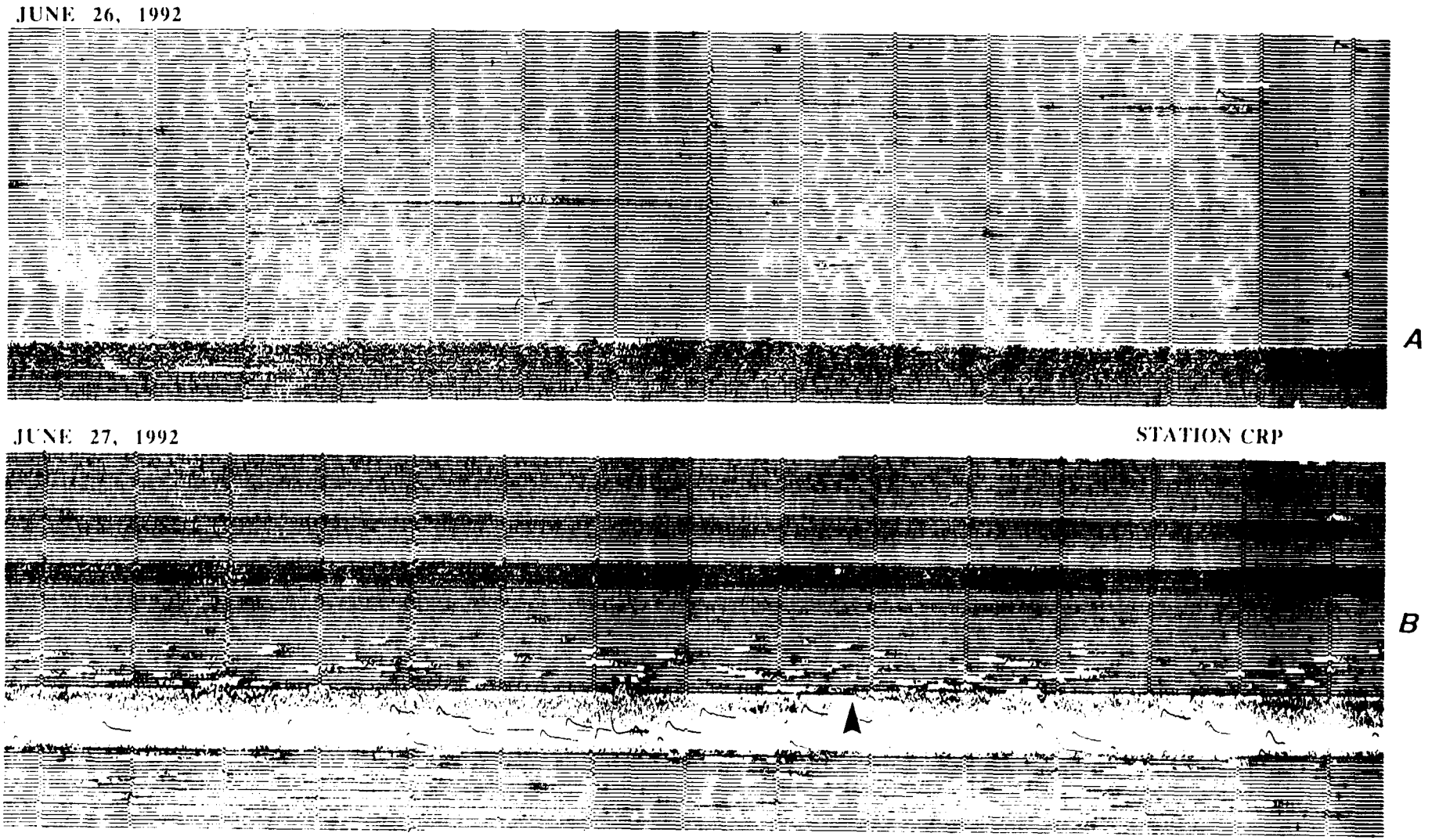

Figure 4. Helicorder records from station CRP, 5 km west of Crater Peak vent on Mount Spurr volcano, southwestern Alaska, for June 26 and 27, 1992. Note (A) continuous tremor starting at 12:03 p.m. ADT (20:03 UT) June 26, and (B) earthquake swarm starting 03:00 a.m. ADT (11:00 UT) June 27. Eruption tremor (arrow) started at 07:04 a.m. ADT (15:04 UT) June 27. Tick marks are at one-minute intervals.

ANALYSES AND RESULTS

We studied (1) duration and energy versus time for all the tremor bursts and the first three episodes of continuous tremor during June 6–27; (2) amplitude ratios for selected tremor bursts (June 8–22) and one episode of continuous tremor on June 24–25; (3) amplitude variations for October 1–6 continuous tremor; (4) spectra for a tremor burst, the June 24–25 tremor episode, a sample of June 26 tremor, and a sample of June 27 tremor during the first eruption; (5) spectral variations for October 1-6 continuous tremor; and (6) a comparison of tremor during eruptions at Mount Spurr with tremor recorded during eruptions at other volcanoes.

DURATION AND ENERGY VERSUS TIME

Tremor bursts began on June 6, 1992, and we tabulated the events and plotted the cumulative duration and cumulative energy as a function of time (fig. 3 and Appendix). We observed that the overall pattern of the plots was concave upward, but individual segments were all concave downward. For example, the cumulative-duration plot was concave downward from June 6 to June 21 (A in fig. 3) indicating that the rate of occurrence of the tremor bursts was decreasing with time. On June 11, a field party observed that the crater lake had changed color from light blue to dark gray, and that adjacent fumaroles had increased in activity (T. Miller and R. McGimsey, oral commun., 1992). These observations and shallow earthquake locations suggested that a change had occurred in the shallow geothermal system, specifically an increase in heat caused by magma intruding to shallow levels in the crust. The concave downward part of figure 3 suggests that the source of heat moved up and stopped, and it gradually lost energy as a function of time. Alternatively, the geothermal system could have used up its supply of water or some other geochemical change could have occurred, such as partial sealing of cracks and pores. The low amplitudes of the tremor bursts (about 1 cm^2 reduced displacement) were in the same range as tremor observed elsewhere in association with hydrothermal activity, lending further evidence to the hypothesis that the tremor bursts probably represented some type of boiling phenomena.

The two 2-hr long tremor episodes on June 24–25 occurred during poor weather, so no direct field observations were made. However, on June 26 a field party observed that the crater lake was half empty, and lithic block impact marks were photographed on the mud of the former lake bottom (C. Nye, oral commun., 1992). The cumulative duration and cumulative energy plots from June 24 to June 26 (B in fig. 3) are also concave downward, suggesting that a heat source (magma) moved upward and stopped, losing its heat or using up the available water. The impact marks suggest that mild phreatic activity may have occurred. The last part of the tremor (C in fig. 3) on June 26 and 27 is also concave downward in energy, but straight in cumulative duration because the same duration of tremor occurred in each 6-hour time step once it became continuous. Inspection of the seismograms in figure 4 shows that the continuous tremor occurred in four bands. In each case the onset was relative abrupt and strong, and the tremor then gradually declined in amplitude over several hours. Each of these four bands follows the same pattern as parts A, B, and *C* in figure 3, again suggesting that the magma moved upward to a shallower level and stopped, losing heat or using up the available water. Following the 4-hr VT earthquake swarm on June 27 (fig. 4) the onset of strong tremor marked the start of the eruption, confirming that magma had indeed moved to shallow levels in the volcano.

AMPLITUDE RATIOS

Except in rare cases when the onset is abrupt (Aki and Koyanagi, 1981), volcanic tremor cannot be routinely located because no clear phases such as P-wave or S-wave arrival times are present in the waveforms. Therefore, indirect techniques are commonly used to infer changing tremor source locations. At Mount Spurr we examined amplitude ratios between near and far stations to determine whether any significant depth changes had occurred. We used data from stations CPK, 400 m from the vent, and CRP, 4.8 km from the vent (fig. 1). The requirement of on-scale seismograms for CPK and good signal-to-noise ratio for CRP restricted our search to only a few samples, yet sufficient data have been analyzed to provide reliable results.

We computed rms (root-mean-square) amplitudes for CPK and CRP data for six samples (table 2) using the program SAC (Tapley and Tull, 1991). Amplitudes for a tremor burst on June 11 and the 2.5-hr episode on June 24–25 at stations CPK and CRP are shown in figure 5. The plots are normalized so that the amplitude on station CRP appears the same (left side, fig. 5), whereas the CPK amplitude varies. We observe that the amplitude ratio CPK/CRP for June 11 is 1.5, and the ratio for June 24–25 is 4. The amplitude on the close station CPK has increased significantly compared with the amplitude at the more distant station CRP. We interpret this as evidence for a shoaling of the depth of the source. Recall that the

Table 2. Root mean square amplitudes of Mount Spurr volcanic tremor.

Date	Time (ADT)	CKN rms amplitude	CPK rms amplitude	CRP rms amplitude	CPK/CRP ratio
June 8	08:20 a.m.	92	63	41	1.5
June 11	07:00 a.m.	199	204	138	1.5
June 17	12:16 a.m.	74	63	50	1.3
June 22	08:44 a.m.	119	141	58	2.4
June 24	04:24 p.m.	44	68	17	4.0

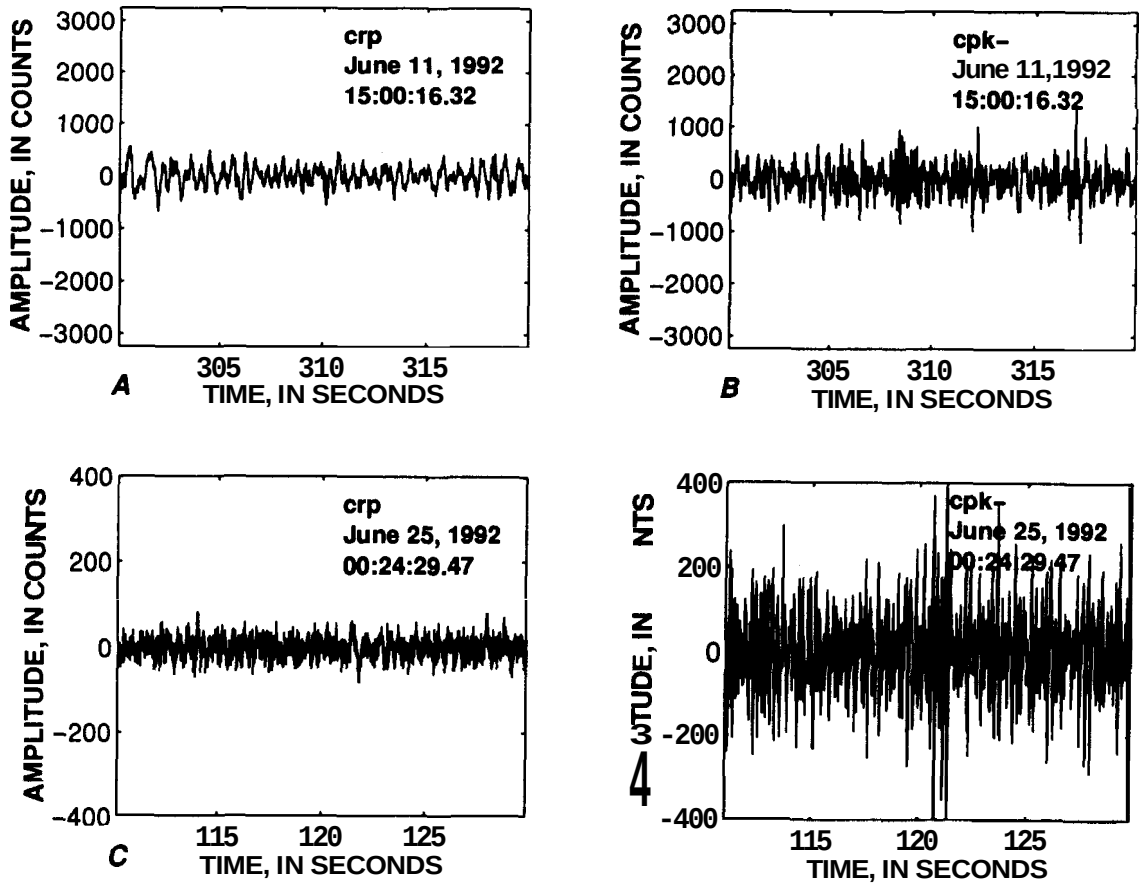

Figure 5. Amplitude ratios for two tremor samples from seismic stations on Mount Spurr volcano, Alaska. For each sample, data from stations CRP *(A* and *C)* and CPK *(B* and *D)* are shown. The plots are normalized to the CRP rms amplitude. The ratio CPK/CRP on June 11 is about 1.5 (compare A and *B),* whereas on June 24–25 the ratio is about 4 (compare *C* and *D).* This suggests that the June 24–25 event occurred closer to station CPK, or at shallower depth since station CPK is located only 400 m from the vent whereas station CRP is located 5 km from the vent. Universal Time.

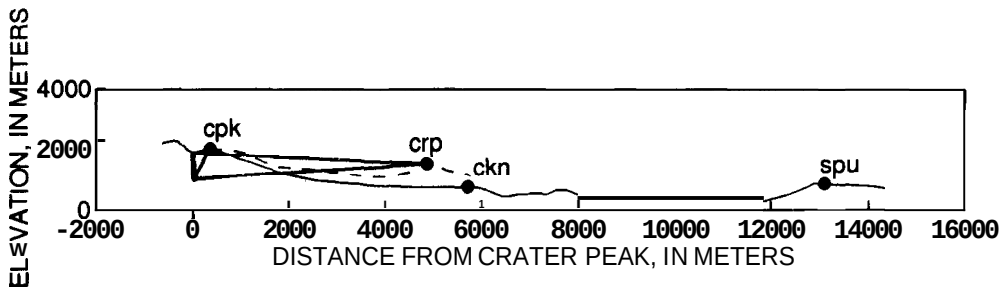

Figure 6. Schematic diagram of postulated depth distribution that explains amplitude ratios shown in figure 5. Two true-scale topographic profiles are shown. Straight line ray paths are drawn to stations CPK and CRP. The rays to station CRP are nearly the same length, whereas those to station CPK are scaled to the changing amplitude ratio. The straight rays to station CRP are unrealistic because of the topography, nevertheless, they illustrate the concept.

crater lake was half empty, with lithic block impacts visible, when it was viewed June 26 prior to the onset of the continuous tremor (Alaska Volcano Observatory, 1993; C. Nye, oral commun., 1992). This observation suggests that mild phreatic activity may have occurred, probably during the June 24–25 tremor episodes.

If we assume a point source at the surface for the June 24–25 tremor, then we can perform a simple inversion for the depth of the tremor burst on June 11. The geometry is shown in figure 6. The distance of the ray path to the distant station CRP (4.8 km) changes very little with a change in source depth, whereas the distance to the close station CPK (400 m) changes significantly. We use the amplitude ratios 1.5 and 4 given above, and assume $1/r$ geometric spreading for body waves (energy decays as $1/r^2$, so amplitude decays as $1/r$). This means the distance must increase by a factor of $4/1.5=2.67$. We assume straight-line ray paths, and use the Pythagorean theorem to solve for the depth change. This yields a depth of 920 m for the June 11 tremor burst. If the June 24–25 source is located at a depth of 100 m rather than at the surface, then the depth of the tremor burst would be 934 m. This calculation is a first-order approximation only (probably reliable to only one significant figure), and it ignores effects such as attenuation, reflections, and refractions. If the source was not deeper but was farther away in some other direction, the distances would be different than those determined above. Also, if the source is a line source or some other geometry, the calculation is more complicated, and it has not yet been attempted.

OCTOBER 1–6 AMPLITUDE VARIATIONS

Volcanic tremor continued for 1 week following the September 17 eruption and ceased on September 25. After a 1-week hiatus, tremor resumed on October 1. The tremor sequence in October showed significant temporal variations, including patterns similar to those that have preceded eruptions at Mount Spurr and elsewhere.

The RSAM plot (fig. 7) shows tremor starting on October 1 and then increasing in amplitude at a nearly exponential rate on October 2, after which it stopped rather abruptly. This episode was similar to the RSAM plot for the days preceding the January 2, 1990, eruption of Redoubt Volcano (Brantley, 1990). On October 3 a series of 5 tremor episodes occurred, each about 1.5 hr long. This signal resembled banded tremor (Kieffer, 1984), and it was also similar to the tremor preceding the June 27 eruption of Mount Spurr. On October 4, tremor returned and the amplitude again increased nearly exponentially. When this tremor declined in amplitude on October 5, another series of tremor episodes occurred, each about 2 hr long, similar to those of October 3, but followed by a gradual decline.

From October 1 through October 6 a steam plume was being emitted from Crater Peak to heights of 2,000 to 12,000 ft above the volcano, and approximately steady amounts of SO_2 and CO_2 gas were being emitted (400 and 2,900 tons/day, respectively). Doukas and Gerlach (this volume) noted a drop in SO_2 flux shortly after the onset of several tremor episodes. There was no clear correlation between plume height and tremor amplitude, and no eruption occurred.

The RSAM plots were valuable for near-real-time monitoring to quickly compare the current tremor level to that of the previous few days and to monitor the temporal patterns. Although the amplitude varied considerably, the tremor was quite stationary in its frequency characteristics and in its relative amplitudes at different stations. We speculate that this tremor was caused by magma degassing at shallow depths.

The tremor observed in October demonstrated that patterns of occurrence alone, such as exponential increases in amplitude or periodic banding, are not sufficient basis for forecasting eruptions.

SPECTRA

We computed Fourier spectra for several representative portions of the tremor data to search for significant spectral peaks that might help identify source properties. We selected a typical tremor burst on June 11, and samples of tremor episodes on June 25, June 26, and during the eruption on June 27 (fig. 2). For each sample, we chose four adjacent windows, each 10 sec long, computed Fast Fourier Transform spectra, then stacked the spectra. This adds stability because constructive interference enhances the real peaks whereas destructive interference diminishes the noise. Results are shown in figure 8. For all the samples, significant spectral amplitudes occur between 0.5 and 5 Hz, and the highest amplitude peaks are near 2 Hz. In detail, however, two of the spectra show something quite remarkable.

If the June 26 spectrum is horizontally compressed and superimposed on the June 27 spectrum, as shown in figure 9, we see that nearly all of the main spectral peaks coincide. The amount of compression is 18 percent. Mori and others (1989) showed a shifting in frequency of a single prominent peak at Langila Volcano in Papua New Guinea, and Kamo and others (1977) showed a series of spectral peaks from Sakurajima Volcano in Japan whose positions changed sys-

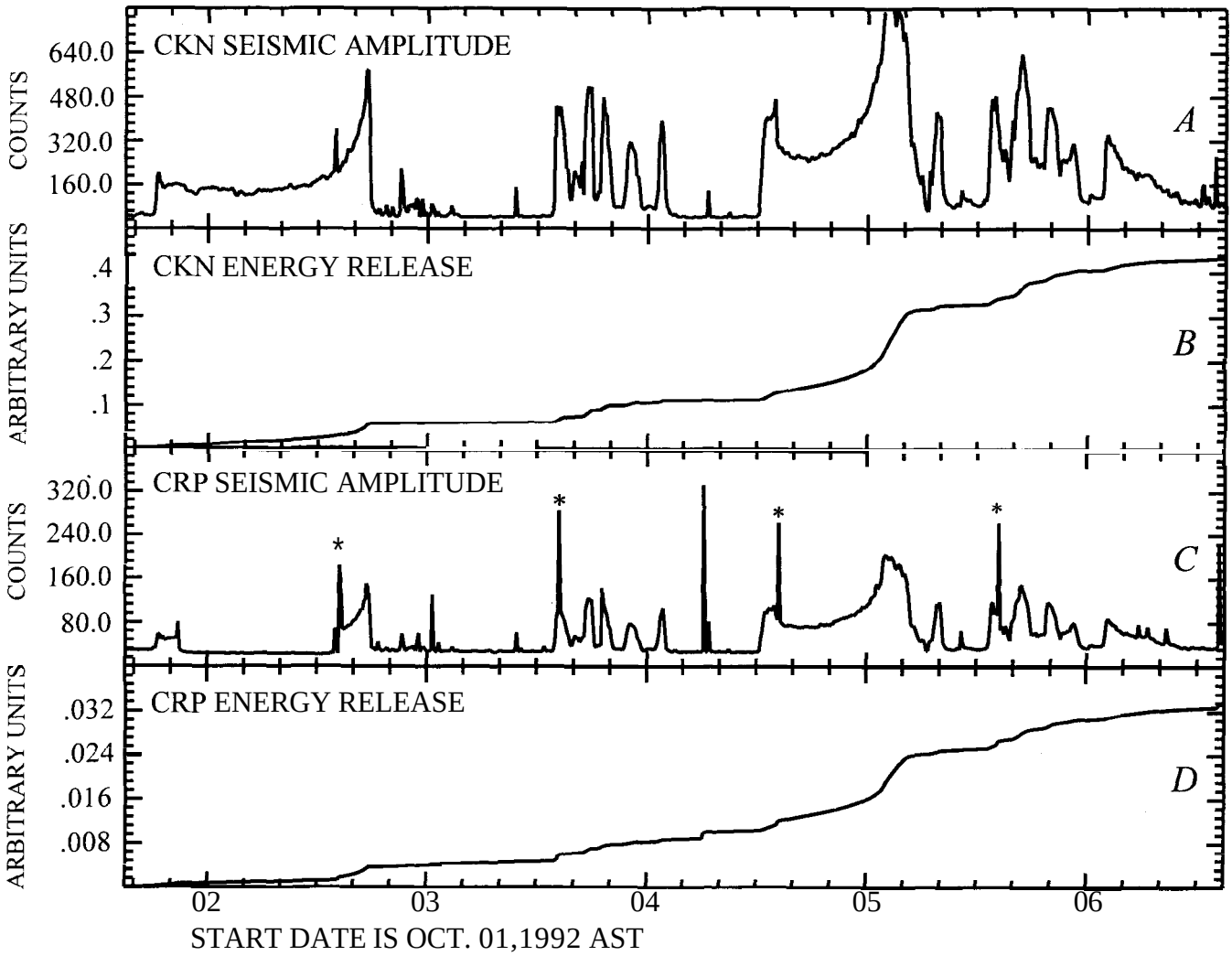

Figure 7. RSAM (Real-time Seismic Amplitude Measurement) plot for tremor data from Mount Spurr volcano, Alaska, for October 1–6, 1992. Horizontal axis is time in days; vertical axis is digital counts for A and C, arbitrary units for B and D. A, amplitude, station CKN; B, cumulative energy release, station CKN; C, amplitude, station CRP; D, cumulative energy release, station CRP. In D on October 2 the signal gain-ranged for part of the time. Equally spaced spikes (asterisks) are daily calibration sequences.

tematically with time. In all three cases the shifting of peaks implies either that the length of a resonator changed by 18 to 40 percent, or that the acoustic wave speed changed, as could happen, for example, with the introduction of bubbles. The presence of even a small amount of bubbles dramatically lowers acoustic speeds of fluids (Kieffer, 1977).

The Mount Spurr data differ from these other data in several significant respects. First, the Mount Spurr eruptive conditions changed from no eruption to vigorous subplinian eruption. The Langila and Sakurajima data, on the other hand, were recorded during times of relatively constant conditions. Second, the Langila case was recorded over 2 minutes, whereas the Spurr data were recorded over 19 hours. Third, the Langila and Sakurajima seismograms appear to be very even and regular, whereas the Spurr data are far more irregular (fig. 2). On closer inspection of figure 9, the Spurr spectra consist of a broadband triangular shaped part (apex upward) from 0.5 to 4 Hz, with evenly-spaced sharp individual peaks superimposed. This has important implications for the source model. The broadband part suggests that a series of random pulses was acting at the source (see Hurst, 1992). These could be, for example, bubble cavitations, flow perturbations, or impacts of blocks on the side of a conduit. The evenly-spaced sharp peaks, on the other hand, suggest resonance modes of an oscillator. The single set of peaks suggests a one-dimensional oscillator, with each of the peaks representing an eigenfrequency of vibration (for example, Schick and others, 1982; Kamo and others, 1977; McNutt, 1986).

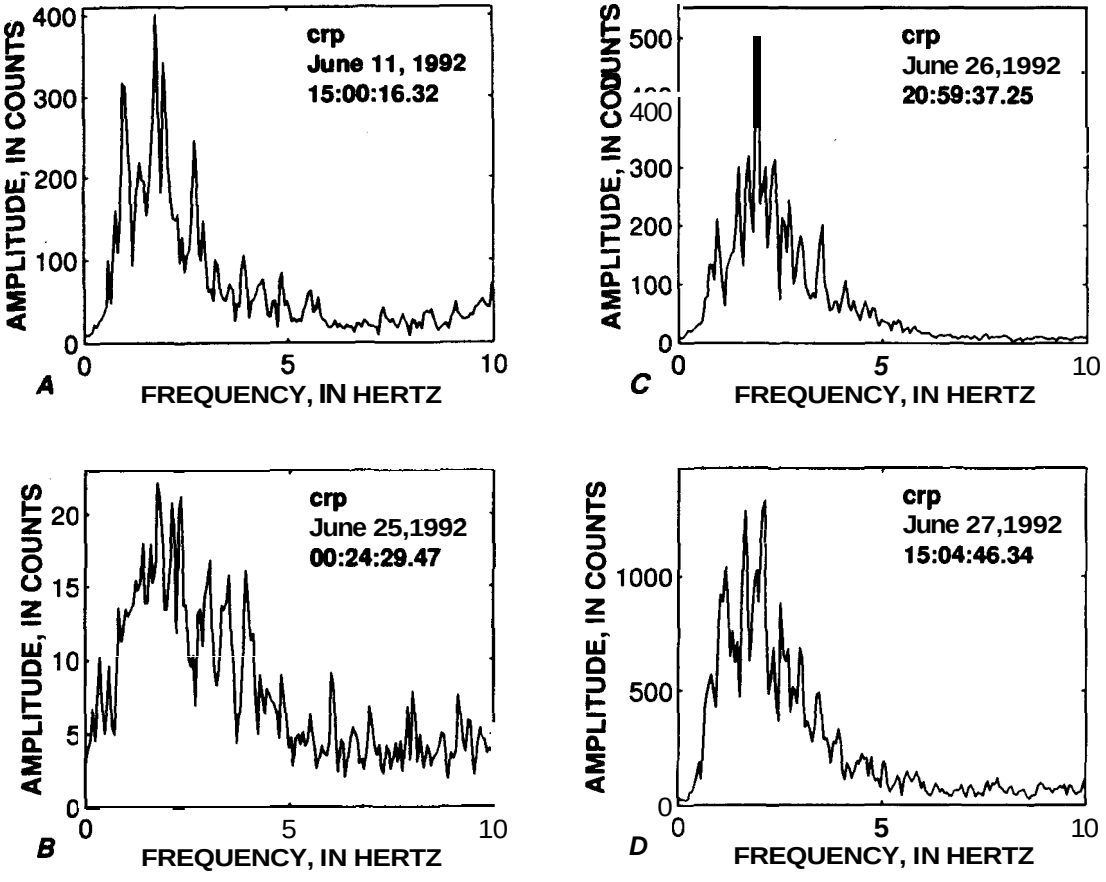

Figure 8. Fourier spectra for the time series shown in figure 2. Each spectrum is a stack of four individual spectra, each for a 10-sec sample of data. A, tremor burst, June 11, 1992. B, tremor episode 154 minutes long, June 24–25, 1992. C, continuous tremor prior to the eruption, June 26, 1992. D, eruption tremor, June 27, 1992. Universal Time.

Models of this type involve a one-dimensional oscillator such as the familiar organ pipe, whose permissible frequencies of resonance are determined by the length, velocity, and boundary conditions. A pipe with two open or two closed ends has resonance modes $n\lambda/2$ (where λ =wavelength and n=1,2,3,...). A pipe with one open end and one closed end has resonance modes $n\lambda/4$ (where λ =wavelength and n=1,3,5,...). In each case the spectral peaks are evenly spaced, however, the spacing from the origin to the first peak is different. The interpeak and origin-to-peak spacing is the same for $n\lambda/2$ modes, whereas the origin-to-peak distance is $\lambda/2$ that of the interpeak distance for $n\lambda/4$ modes. This feature provides a simple way to identify modes on a spectrum.

The data suggest that both sets of modes are present in spectra from June 26 and June 27, before and during the eruption. The peaks on figure 9 have been numbered for identification, and we observe that alternate peaks change amplitudes systematically from before to during the eruption. Peaks 1, 3, 5, 7, and 9 had the same or only slightly different amplitudes, whereas peaks 2, 4, 6, 8 and 10 became significantly larger during the eruption. The pattern is most clear for peaks 1, 2, 3, and 4. The most straightforward interpretation for this pattern is that there was a change in the boundary conditions. We suggest that the spectral peaks represent mixed modes of organ pipe vibration, that is, both open-ended and close-ended modes are present. If the boundary conditions are changed, for example by breaking an impermeable cap, changing the shape, or transmitting lava, then one set of modes would be enhanced relative to the other. It is best to think of the boundary conditions in terms of reflection and transmission, rather than open-ended or close-ended. However, the open-ended and close-ended modes give a clear conceptual picture. We observe that the close-ended modes (that is, one open end and one closed end) became stronger during the eruption, which is what would be expected as the vent is reamed out. Although preliminary, to the best of our knowledge, this is the first observation of this type that has

been made on volcanic tremor spectra. This is also a clear source effect. The fundamental mode for the even-numbered peaks (closed-end modes) does not appear on figure 9 because its frequency is too low to be recorded on the 1-Hz seismometer we used.

While we have presented our preferred preliminary model, other possibilities exist. The shape of a resonator could have changed, for example from a one-dimensional pipe-like structure to a two-dimensional rectangular crack (Chouet, 1992), and the systematic variation of spectral amplitudes could be caused by preferential excitation of modes in one direction over the other. It is also possible that no resonator was involved, and that the observed amplitude variation is caused by some other process (Julian, 1994). It is conceivable that the alternate peak spectral amplitude variations are due to chance alone, however, we think that it is very unlikely that random fluctuations would be so systematic.

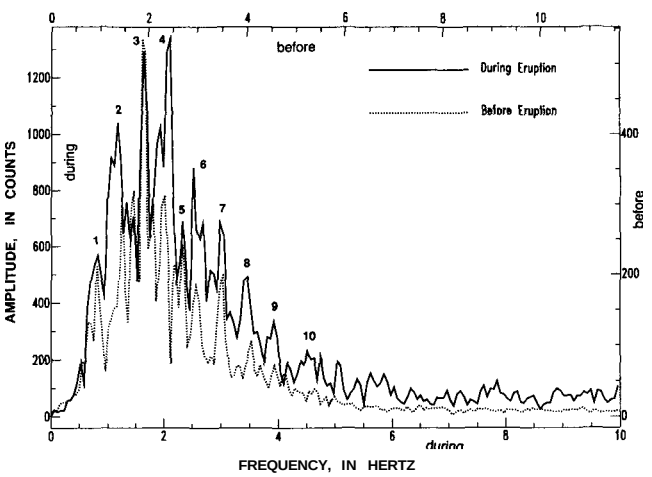

Figure 9. Spectra from figure 8C and 8D superimposed with the horizontal axis compressed by 18 percent for the June 26 spectrum, Left and bottom scales refer to tremor during the eruption on June 27. Top and right scales refer to pre-eruption tremor on June 26. Peaks numbered for reference.

OCTOBER 1–6 SPECTRAL MEASUREMENTS

In addition to computation of spectra for selected tremor samples as discussed above, we also studied spectra using SSAM (Stephens and others, 1994). SSAM runs continuously in the background, and plots can be made at any time for stations and times of interest. SSAM plots show spectral amplitudes in predetermined bands that are several tenths of a Hertz wide. SSAM is thus a good tool to use when the spectra do not vary with time, but it lacks the resolution to identify small changes in spectral position.

The SSAM plot (fig. 10) shows data from October 2–6, the same period as figure 7. Here we see persistent high amplitudes in the 1.9 to 2.5 Hz bands, the same frequencies that are high amplitude in the spectra shown in figure 8. We also observe that as the signal becomes stronger (fig. 7), the spectral content becomes somewhat more broadband. This may be partially caused, however, by saturation of the spectral bands for strong signals. In general, the spectral content is remarkably uniform over the period October 2–6. Based on the results of both RSAM and SSAM, we conclude that volcanic tremor with a single source occurred during October 1992. Our preliminary conclusion is that shallow-level degassing of magma was the source. It is not known whether the degassing was juvenile, hydrothermal, or a mixture of the two, although we suggest the latter was the more likely gas source (Doukas and Gerlach, this volume).

Tremor occurred again for several hours on November 9–10 in association with a swarm of shallow earthquakes. This tremor was observed mainly on the closest station CP2 (a replacement for CPK, fig. 1) and consisted of a high signal level recorded between discrete events of the earthquake swarm. The frequency content of this tremor was somewhat higher than that of previous tremor (>5 Hz). No detailed analyses have yet been carried out on this tremor.

TREMOR DURING ERUPTIONS

Time histories for the three eruptions using RSAM data for station BGL, which operated continuously during all three eruptions, are shown in figure 11. Station BGL has a 1-sec vertical geophone, and it is located 7.7 km west of the Crater Peak vent (fig. 1). Because the station is fairly close to the vent, its data are partially saturated (clipped), especially for higher amplitudes above 1,200 counts. The total durations and volumes of each eruption are shown in table 1. However, the duration of the strongest eruption tremor was roughly proportional to the tephra volume of each eruption. For example, the duration of tremor greater than 800 counts on June 27 was 1 hour, on August 18 about 2.8 hours, and on September 16–17 about 2.5 hours (recall that the end of the September eruption was "contaminated" by an earthquake swarm), whereas the tephra volumes were 44, 52, and 56 million cubic meters, respectively.

The amplitude of Mount Spurr eruption tremor is compared to that from eruptions at other volcanoes in figure 12 (modified from McNutt, 1994). Representative values from the June 27 and August 18 eruptions are shown; the maximum amplitude during the August eruption was approximately double the June

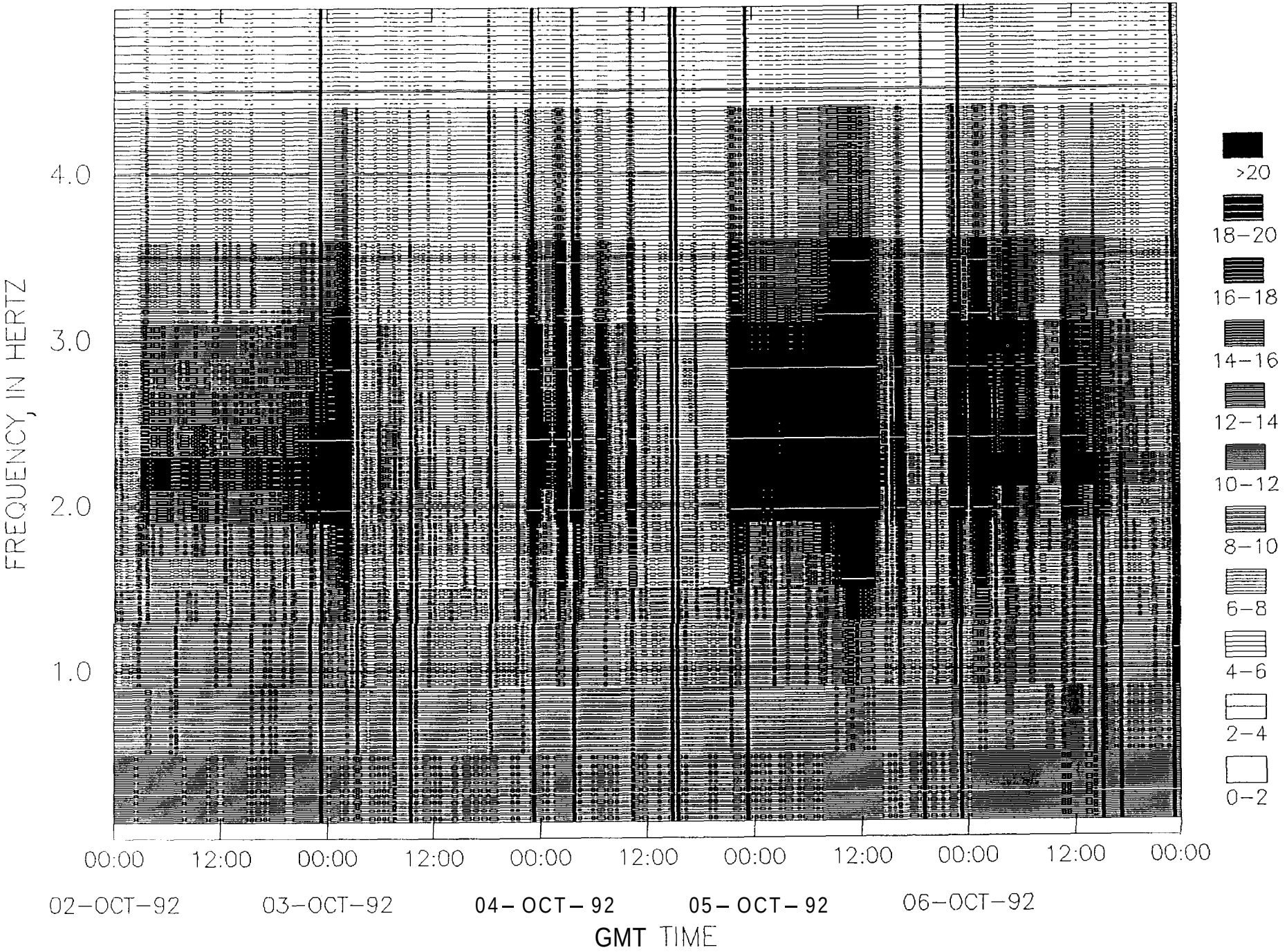

Figure 10. SSAM (Seismic Spectral Amplitude Measurement) record for October 2–6, 1992, for station CRP on Mount Spurr volcano, Alaska, plotted with high values in 18-minute cells. Spectral amplitudes are shown as various shades and patterns, with darker colors representing higher amplitudes. Frequency bands are 0.2 Hz wide. Note persistent high amplitudes in the 1.9 to 3.2 Hz bands.

maximum. Each datum represents the tremor amplitude normalized to reduced displacement, which corrects for distance, geometric spreading, and instrument magnification (Aki and Koyanagi, 1981; Fehler, 1983), and is plotted versus the Volcanic Explosivity Index (VEI) of Newhall and Self (1982). Each of the three main eruptions of Mount Spurr were VEI=3, as determined from tephra volumes (table 1) and ash-column heights of 9 to 15 km. The Mount Spurr tremor amplitudes are similar to values obtained elsewhere for eruptions of similar size, although this does not imply that the exact eruption mechanisms were identical. The mechanisms of the Mount Spurr eruptions are discussed by Neal and others (this volume), and they are characterized as subplinian.

The amplitude of a representative tremor burst from June 11 is also shown in figure 12 for comparison. The VEI was set at 0 because of the less than 1 km steam plume and the impact block craters in the mud flat within a few tens of meters of the vent. This value also falls in the range observed at other volcanoes for eruptions of similar size and characteristics (Gil Cruz and others, 1987; Leet, 1988; McNutt, 1994).

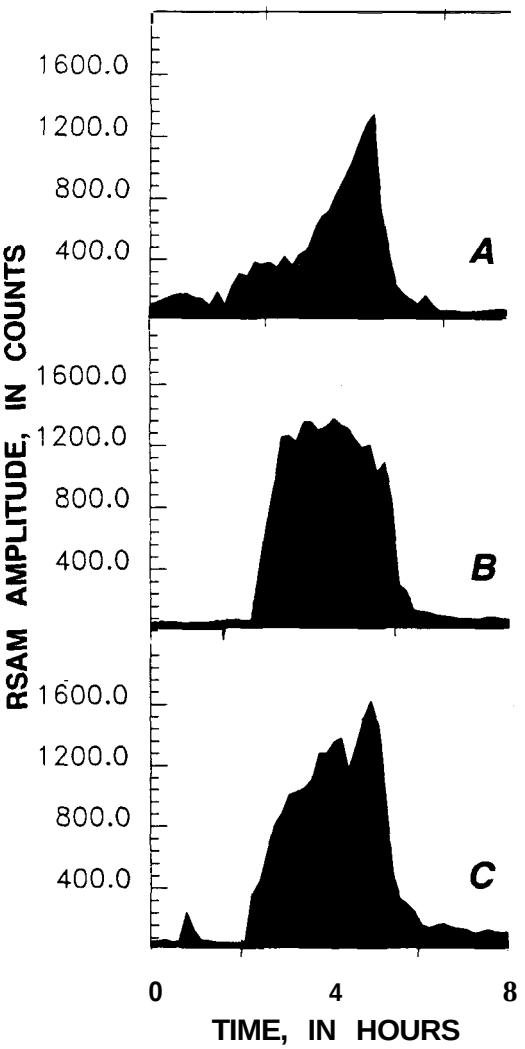

Figure 11. RSAM (Real-time Seismic Amplitude Measurement) plot for volcanic tremor amplitudes during the three 1992 eruptions of Mount Spurr in southwestern Alaska. Station BGL is located 7.7 km west of Crater Peak, the active vent. Vertical axis is digital counts. Partial saturation of highest amplitudes (above 1200 counts) occurred during all three eruptions. *A*, June 27; B, August 18; *C*, September 16–17.

DISCUSSION AND CONCLUSIONS

We used a variety of methods to study tremor at Mount Spurr, choosing specific techniques for different time periods based on station operation, signal strength, and overall data sufficiency. In this section, we synthesize the key results into a preliminary qualitative model of tremor generation.

The tremor bursts first appeared on June 6, the day after the highest daily number of volcano-tectonic (VT) earthquakes, 28 events on June 5 (Power and others, this volume), of the 9.5-month swarm up to that time. During the three weeks over which tremor bursts were observed, the seismicity remained at about 5 to 10 locatable VT earthquakes per day. This suggests that magma or volatiles had reached shallow levels in the crust, and instead of building up stresses and triggering VT earthquakes, the magma or volatiles interacted with ground water to produce tremor bursts. Recall that geochemical changes were observed in the crater lake shortly after the tremor bursts first appeared. For 18 days the cumulative duration and cumulative energy plots were concave downward (fig. 3), which means that the rates of tremor occurrence and energy were declining with time. Amplitudes were small (about 1 cm^2 reduced displacement) and source depth was about 1 km. We infer that magmatic heat was interacting with the shallow geothermal system.

A significant change occurred on June 24–25 when a 2.5-hour tremor episode occurred, followed by another similar episode 12 hours later (fig. 3 and Appendix). The durations and energies of these two episodes alone exceeded those of all the earlier bursts together. The source was becoming shallower, as indicated by changing amplitude ratios (figs. 5 and 6) and the crater lake was partially emptied, with lithic block impact marks visible. The next significant change was the onset of continuous tremor 19 hours before the first eruption. The cumulative duration increased again by a factor of about 3, the cumulative energy also increased by a factor of 3 (fig. 3), and the source remained shallow. Evenly-spaced, narrow spectral peaks suggest that a one-dimensional resonator (pipe or con-

duit) was active at this time. We believe the conduit was filled with a mixture of water, lithic materials, magma, and magmatic fluids. The concave downward parts of the energy plot and the similar amplitude patterns on seismograms (figs. 3 and 4) suggest that heating and upward movement occurred intermittently and abruptly, rather than smoothly and steadily.

The onset of a shallow (1 to 2 km beneath the vent) VT earthquake swarm preceded the first eruption by 4 hours (Power and others, this volume); the onset suggests that stresses were again building up as magma made its final ascent to the surface. Tremor was constant and of low amplitude during this swarm. We speculate this means that all the fluids had been boiled off by this time. The eruption began quite abruptly and the tremor looked much the same as tremor recorded previously except that it was stronger by a factor of two. Spectra computed for tremor during the eruption showed the same peaks shifted in frequency by 18 percent. The presence of the same peaks implies that the same structure was active; namely, the conduit previously occupied mainly by water or a water-rich mixture was now occupied mainly by magma. The shifting of the spectral peaks to lower frequencies (fig. 9) suggests that either the resonator (conduit) length increased or the acoustic velocity decreased within the conduit. Either hypothesis is reasonable and we cannot yet distinguish between these possibilities. The systematic change in amplitudes of alternate spectral peaks (fig. 9) suggests that boundary conditions changed from closed (reflection) to open (transmission) at one end of the conduit from before to during the eruption. This observation is consistent with disruption of an impermeable cap at the top of the conduit during the initial stages of the eruption. Tremor during the eruptions was stronger than any previous tremor and was similar in strength (16 to 30 cm^2 reduced displacement) to that recorded at other volcanoes (fig. 12).

All three eruptions were similar to each other in their durations, volumes, ash-column heights, chemistry, and other parameters (table 1, fig. 11; Alaska Volcano Observatory, 1993). Tremor during the eruptions was also similar. However, patterns of tremor occurrence before and after the eruptions varied considerably. In June, most tremor preceded the eruption; we suggest that this tremor was chiefly hydrothermal in origin. No tremor followed the June eruption. In August, only a single short tremor episode occurred about 1 hour before the eruption. We suggest that the hydrothermal system had not yet been fully re-established, or had been re-established with different geometry or boundary conditions. In September, weak tremor occurred for 3 hours before the eruption, but in contrast to June and August, tremor occurred after the eruption continuously for 1 week. Because the hydrothermal system had been seriously perturbed by the eruption, we suggest that continued degassing of unerupted shallow magma was the source of this tremor. Similar conditions and tremor occurred from October 1 to 20. The last tremor on November 9–10 may be different than most other tremor at Mount Spurr; its frequency content was higher and its amplitude distribution between stations was different. However, thorough analyses of this last tremor are not yet complete.

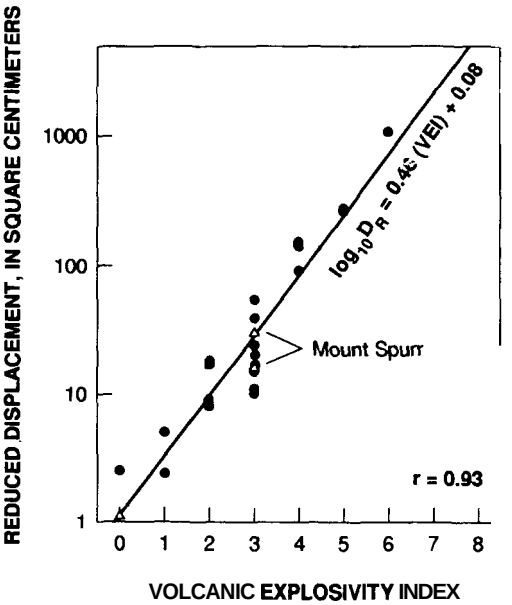

Figure 12. Volcanic tremor reduced displacement versus the Volcanic Explosivity Index (VEI) of Newhall and Self (1982). Data represent 24 eruptions at 15 different volcanoes. The plotted line is a linear regression fit to the data excluding Mount Spurr volcano in southwestern Alaska and has a correlation coefficient r of 0.93. Representative values from the June 27 and August 18 eruptions of Mount Spurr, and from a tremor burst, shown as triangles. Modified from McNutt (1994).

Several of the observations made during this preliminary work have implications for our monitoring efforts. For example, spectra are routinely computed for tremor and there are many published examples in the literature. Nevertheless, our observation of the systematic change in the amplitude of alternate peaks appears to be unique and we are not aware of any published examples. This is clearly a source effect, and it may be possible to exploit this feature in the future to improve eruption forecasting. The shifting of the spectral peaks has been observed elsewhere, but the Mount Spurr observations occurred over a longer time scale and when eruption conditions had clearly changed. Future analyses will elucidate the timing more precisely. SSAM was not useful for determining the

shifting of the spectral peaks and the amplitude variations of alternate peaks because the frequency bins were fixed and did not coincide with the spectral peaks.

Several of our most important observations depended on data from individual seismic stations. Station CPK, which was located only 400 meters from the vent, proved to be especially valuable. This station enabled us to identify the occurrence of tremor bursts in early June when they were small enough that they were not clearly recognized on more distant stations. This station also enabled us to determine dramatic changes in the rms amplitude ratios (fig. 5), which we believe were most likely caused by a shoaling of the, source. The station CPK was destroyed twice during eruptions, and its replacement was worth the cost because of the insight into physical characteristics of tremor we obtained from this key station. We suggest that every monitored volcano would benefit from having at least one station within a few hundred meters of the active vent.

Our analyses and monitoring efforts greatly benefited from having a variety of tools at our disposal, including helicorders, continuous digital data, event-triggered data, RSAM, and SSAM. Our experience in forecasting eruptions at Mount Spurr illustrates the importance of closely monitoring volcanic tremor using a variety of techniques and methods. Future work at Mount Spurr will focus not only on more detailed analyses of the data presented here, but also on improvements in the methods for recording and analyzing tremor in general.

REFERENCES CITED

Aki, K. and Koyanagi, R.Y., 1981, Deep volcanic tremor and magma ascent mechanism under Kilauea, Hawaii: Journal of Geophysical Research, v. 86, p. 7095–7110.

Alaska Volcano Observatory, 1993, Mt. Spurr's 1992 Eruptions: Eos, Transactions of the American Geophysical Union, v. 74, no. 19, p. 217 and 221–222.

Brantley, S.R., 1990, The eruption of Redoubt volcano, Alaska, December 14, 1989 – August 31, 1990: U.S. Geological Survey Circular 1061, 33 p.

Chouet, B., 1992, A seismic model for the source of long-period events and harmonic tremor, in Gasparini, P., Scarpa, R., and Aki, K., eds., Volcanic Seismology, IAVCEI Proceedings in Volcanology, v. 3, Berlin, Springer-Verlag, p. 133–156.

Chouet, B.A., Page, R.A., Stephens, C.D., Lahr, J.C., and Power, J.A., 1994, Precursory swarms of long-period events at Redoubt Volcano (1989–1990), Alaska: Their origin and use as a forecasting tool: Journal of Volcanology and Geothermal Research, v. 62, p. 95–135.

Dawson, P.B., Chouet, B.A., Lahr, J.C., and Page, R.A., 1992, Spatial relationship between LP earthquakes and a shallow three-dimensional velocity anomaly beneath Redoubt Volcano, Alaska: Eos (American Geophysical Union Transactions) supplement, v.73, p. 343.

Endo, E.T., and Murray, T.L., 1991, Real-time Seismic Amplitude Measurement (RSAM): a volcano monitoring and prediction tool: Bulletin of Volcanology, v. 53, p. 533–545.

Fehler, M., 1983, Observations of volcanic tremor at Mount St. Helens volcano: Journal of Geophysical Research, v. 88, p. 3476-3484.

Gil Cruz, F., Meyer, H., Chouet, B., and Harlow, D.H., 1987, Observations of long-period events and tremor at Nevado del Ruiz volcano 1985–1986: Abstract volume, Hawaii Symposium on How Volcanoes Work, Hilo, Hawaii, p. 90.

Gordeev, E.I., 1992, Modeling of volcanic tremor wave fields: Journal of Volcanology and Geothermal Research, v. 51, p. 145–160.

Hill, D.P., Ellsworth, W.L., Johnston, M.J.S., Langbein, J.O., Oppenheimer, D.H., Pitt, A.M., Reasenberg, P.A., Sorey, M.L., and McNutt, S.R., 1990, The 1989 earthquake swarm beneath Mammoth Mountain, California: An initial look at the 4 May through 30 September activity: Seismological Society of America Bulletin, v. 80, p. 325–339.

Hurst, A.W., 1992, Stochastic simulation of volcanic tremor from Ruapehu: Journal of Volcanology and Geothermal Research, v. 51, p. 185–198.

Julian, B.R., 1994, Volcanic tremor: Nonlinear excitation by fluid flow: Journal of Geophysical Research, v. 99, p. 11,859–11,878.

Kamo, K., Furuzawa, T., and Akamatsu, J., 1977, Some natures of volcanic microtremors at the Sakurajima volcano: Bulletin of the Volcanological Society of Japan, v. 22, p. 41–58.

Kieffer, S.W., 1977, Sound speed in liquid-gas mixtures: water-air and water-steam: Journal of Geophysical Research, v. 82, p. 2895–2904.

———1984, Seismicity at Old Faithful Geyser: An isolated source of geothermal noise and possible analogue of volcanic seismicity: Journal of Volcanology and Geothermal Research, v. 22, p. 59–95.

Lee, W.H.K., 1989, Toolbox for seismic data acquisition, processing, and analysis: IASPEI Software Library Volume 1, Seismological Society of America, El Cerrito, Calif.

Leet, R.C., 1988, Saturated and subcooled hydrothermal boiling in groundwater flow channels as a source of harmonic tremor: Journal of Geophysical Research, v. 93, p. 4835–4849.

McKee, C., Wallace, D.A., Almond, R.A., and Talai, B., 1981, Fatal hydroeruption of Karkar volcano in 1979: Development of a maar-like crater, in Johnson, R.W., ed., Cooke-Ravian Volume of Volcanological Papers: Geological Survey of Papua New Guinea, Memoir 10, p. 63–84.

McNutt, S.R., 1986, Observations and analysis of b-type earthquakes, explosions, and volcanic tremor at Pavlof volcano, Alaska: Bulletin of the Seismological Society of America, v. 76, p. 153–175.

———1992, Volcanic tremor: Encyclopedia of Earth System Sciences, San Diego, Calif., Academic Press, v. 4, p. 417–425.

———1994, Volcanic tremor amplitude correlated with eruption explosivity and its potential use in determining ash hazards to aviation: U.S. Geological Survey Bulletin 2047, p. 377–385.

Montalto, A., Distefano, G., and Patane, G., 1992, Seismic patterns and fluid-dynamic features preceding the January 15, 1990 eruptive paroxysm on Mt. Etna (Italy): Journal of Volcanology and Geothermal Research, v. 51, p. 133–143.

Mori, J., Patia, H., McKee, C., Itikarai, I., Lowenstein, P., De Saint Ours, P., and Talai, B., 1989, Seismicity associated with the eruptive activity at Langila volcano, Papua New Guinea: Journal of Volcanology and Geothermal Research, v. 38, p. 243–255.

Newhall, C.G., and Self, S., 1982, The volcano explosivity index

(VEI): An estimate of explosive magnitude for historical volcanism: Journal of Geophysical Research, v. 87, p. 1231–1238.

Schick, R., Lombardo, G., and Patane, G., 1982, Volcanic tremors and shocks associated with eruptions at Etna (Sicily), September 1980: Journal of Volcanology and Geothermal Research, v. 14, p. 261–279.

Sonnafrank, G.H.C., Power, J., March, G., and Davies, J.N., 1991, Acquisition and automatic processing of seismic data at the Geophysical Institute, University of Alaska: Seismological Research Letters, v. 62, p. 23.

Stephens, C.D., Chouet, B.A., Page, R.A., Lahr, J.C., and Power, J.A., 1994, Seismological aspects of the 1989–1990 eruptions at Redoubt Volcano, Alaska: The SSAM perspective: Journal of Volcanology and Geothermal Research, v. *62*, p. 153–182.

Tapley, W.C., and Tull, J.E., 1991, SAC—Seismic Analysis Code—Users Manual: Lawrence Livermore National Laboratory, Livermore, Calif.

Ukawa, M., 1993, Excitation mechanism of large-amplitude volcanic tremor associated with the 1989 Ito-oki submarine eruption, central Japan: Journal of Volcanology and Geothermal Research, v. 55, p. 33–50.

Appendix 1. Tremor bursts measured at seismic stations CPK and CRP between June 6 and June 26, 1992, Mount Spurr volcano, Alaska.

[All dates expressed in Universal Time; duration expressed in seconds; amplitude expressed in millimeters]

Time (UT)	CPK duration (sec)	CRP amplitude (mm)
June 6, 1992		
15:00	190	5.5
16:57	130	4.0
18:16	80	5.0
20:43	90	3.5
22:04	160	2.5
June 7, 1992		
01:26	190	1.5
02:28	130	5.0
04:58	220	3.0
05:47	80	3.5
07:26	180	2.5
08:23	200	2.0
09:40	170	2.5
10:58	180	1.5
11:56	180	1.0
13:38	190	4.0
14:04	100	1.0
14:47	200	3.0
15:29	110	3.5
15:48	140	3.0
16:06	110	2.5
18:24	140	3.5
19:01	170	2.5
19:35	140	1.0
June 8, 1992		
06:30	320	3.0
07:58	310	1.0
6/8/92		
09:38	250	5.5
09:46	80	1.5
10:24	240	4.0
11:00	120	1.0
11:36	130	3.5
12:02	100	2.0
12:35	90	3.0
12:52	80	2.0
14:17	130	2.0
15:04	170	1.5
15:53	160	1.5
17:13	170	3.0
17:40	170	2.0
18:28	130	1.5
19:52	180	5.0
21:38	>150	5.0
June 9, 1992		
00:58	270	5.0
01:16	220	6.0
01:26	−150	2.0
02:02	80	4.0
02:37	100	3.0
03:22	90	3.0
04:55	190	4.0
	>120	2.5
15:49	160	1.5
16:02	180	2.5
16:33	80	2.0
18:07	150	2.0
20:29	170	3.5
22:15	140	3.5
June 10, 1992		
01:01	160	4.0
03:04	190	2.0
04:56	250	6.0
05:03	140	2.0
06:12	130	8.0
07:19	90	2.0
08:28	160	3.0
08:41	160	2.0
10:54	120	6.0
11:39	110	5.0
13:04	170	7.0
14:09	150	6.0
15:25	70	1.5
15:31	120	5.0
15:44	110	3.0
16:55	70	3.0
17:09	150	3.0
17:20	160	2.0
19:38	110	1.5
20:43	190	5.0
21:52	230	6.0
June 11, 1992		
00:16	100	4.0
00:31	70	3.0
00:35	140	2.5
00:45	180	1.5
02:53	180	1.5
03:48	100	2.5
03:50	110	2.5
04:39	100	10.0
07:05	70	2.0
07:29	150	3.0
14:26	120	2.0
14:45	150	2.0
15:03	230	5.0
16:07	100	2.0
17:15	>90	1.5
17:18	100	4.0
18:09	120	4.0
18:33	240	2.0
20:04	90	3.5
21:07	220	3.5
21:34	90	2.5
21:36	110	3.0
22:08	110	3.5
23:47	110	3.5
June 12, 1992		
01:01	230	1.0
03:17	250	6.0
05:59	180	2.0
06:25	220	1.5
10:49	240	2.5
11:04	200	2.5
11:12	80	2.5
15:10	130	3.0
15:23	180	1.0
20:47	360	4.0
21:00	220	4.0
21:08	80	4.0
June 13, 1992		
00:15	200	3.0
00:45	210	22.
09:27	190	2.5
09:30	110	2.0
09:43	150	1.5
10:09	120	1.0
10:29	70	1.5
11:29	150	3.0
15:03	230	1.5
18:04	120	3.5
23:10	100	2.0
23:39	120	1.0
June 14,1992		
04:19	100	3.0
06:24	200	3.0
09:00	120	2.0
09:39	110	1.0
16:32	80	1.5
17:39	90	3.5
June 15,1992		
00:08	260	1.5
04:05	90	5.0
12:48	160	<1.0
13:16	120	1.0
13:50	150	1.5
14:04	70	1.0
19:24	100	6.0
June 16,1992		
08:44	250	1.0
17:39	230	3.0
20:50	90	0.0
June 17,1992		
20:16	110	3.5
June 18,1992		
14:07	120	2.0
June 19,1992		
04:57	370	5.0
18:35	260	2.0
19:08	110	4.0
19:36	180	2.0
20:02	360	3.5
June 20,1992		
10:54	220	<1.0
20:59	550	12.0
June 21,1992		
23:05	130	2.0
June 22,1992		
03:25	320	3.5
03:50	80	<1.0
05:49	110	3.0
07:19	270	2.0
08:35	130	2.0
09:29	210	2.0
09:47	100	2.0
16:45	600	6.0
22:16	370	1.5
22:47	190	3.5
June 23,1992		
14:28	220	6.5
22:06	80	10.5
22:09	210	5.0
22:33	170	3.5
June 24,1992		
06:01	260	5.0
15:09	350	6.5
23:34	9,240	5.0
June 25,1992		
06:52	350	5.0
11:13	310	5.5
11:32	8,520	4.5
15:58	240	7.5
20:11	130	9.0
23:55	360	7.0
June 26,1992		
04:51	450	10.
05:36	150	2.0
11:16	390	3.5
20:03	68,460	−10.0